**Virtual Concept Workshop 2016**
**Major Trends in Product Design, Bordeaux, 17th-18th, March 2016**

# PRELIMINARY DESIGN OF A TRANSPARENT TRANSPIRED COLLECTOR

Guy Clarence SEMASSOU [1], Clotilde GUIDI [2], Chakirou TOUKOUROU [3], Henri HOUNKPATIN [4], Stéphan Hallé [5], Antoine VIANOU [6], Gérard DEGAN [7]

**(1) :** Laboratoire d'Energétique et de Mécanique Appliquée (LEMA), Université d'Abomey-Calavi, 01 BP 2009 Cotonou, Bénin

*Phone :* (00229) 95 56 27 98 / (00229) 67 59 03 21 ; *Fax* : (00229) 21 36 01 99

*E-mail :* {**(1)** : seclar2001@yahoo.fr , **(2)** : guiclot@yahoo.fr; **(3)**: potemat@yahoo.fr; **(4)**: orestahenrius@gmail.com; **(5)** : gerdegan@yahoo.fr}

**(5):** DutilTechnologies of Energy and Energy Efficiency Industrial Research Chair (t3e), Department of Mechanical Engineering, École de Technologie Supérieure,Université du Québec 1100, Notre-Dame Street West, Montreal H3C 1K3, Canada

*Phone:* 514 396 8800; *Fax:* 514 396 8950

*E-mail:* stephane.halle@etsmtl.ca

**(6) :** Laboratoire de Caractérisation Thermophysique des Matériaux et d'Appropriation Energétique (LABO-C. T. M. A. E.), Université d'Abomey-Calavi, 01 BP 2009 Cotonou, Bénin

*Phone :* (00229) 95 05 43 93 ; *Fax* : (00229) 21 36 01 99

*E-mail :* avianou@yahoo.fr

## Abstract

Interest in solar air heating is in full recrudescence. Applications can be many and varied wherever the need is created to heat and ventilate the old or new premises, ensure crop drying, or industrial drying, etc. This new interest has led for several years by the appearance on the market of a fair number of systems, including the Transparent Transpired Collector (TTC). The present work presents the description of physical phenomena that govern the operation of the TTC as well as a formulation of these by heat balances. Moreover, order to maximize the collector efficiency and minimizing the temperature difference between the incoming air and the outgoing air, an optimization was carried out using the design variables such as the hole diameter and hole pitch.

**Key words**: Transparent Transpired Collector, transmissivity, absorptivity, emissivity, solar wall.

## 1- Introduction

The growth in global energy demand has been continuing since and despite some crises it accelerated over the past three decades to meet the needs of so-called emerging countries **[G1]**. Indeed, considering only the decade 2001-2011, world energy consumption increased from 9.434 billion tons of oil equivalent to 12 275, ie an increase of nearly 23% **[B1]**. But much of energy used (over 80%) originates from carbon fossil fuel deposits (coal, oil, gas) **[S1]**. These deposits formed over the ages are obviously in limited quantities; they are depletable. The imminent depletion of these resources combined with global warming occasioned their combustion leads us to consider the imperative and efficient use of renewable resources. The resource that is interested in this study is the solar for her thermal applications. Among the most widespread technologies to capture the active solar energy in the building, one can distinguish the solar heating system air unglazed perforated plate sometimes called Unglazed Transpired Collector (UTC) and the Transparent Transpired Collector (TTC). But unlike the UTC which is used for decades to preheat the air in buildings, the TTC is a new generation of solar heating system of air recently appeared on the market. Very little work has been done on the TTC. One can quote for example the works of Badache and al. **[BH1]** which consists in search through all parameters that can influence the performance of TTC, those who have the dominant effect. Description of physical phenomena characterizing the TTC as well as a formulation of these by heat balances were subject of the work of **[G1]**.

The specificity of this study is at first to study the TTC every hour of the day to find the optimal combinations of design variables (hole diameter and hole pitch) that maximize the collector efficiency and minimize the difference temperature between the incoming air and the outgoing air as a sensor is particularly effective when operating at a temperature close to ambient temperature. Desirability functions are put to use in order to maximize the global objective function that will

 

get the candidate solutions. A simulation program including heat transfer equations and energy was developed under MATALAB.

## 2- Materials and methods

### 2.1-Collector configuration

The configuration of the UTC under analysis is illustrated in Figure 1. The collector, mounted vertically, has a perforated absorber and a back wall. The perforated glazing is constituted of polycarbonate and it has been the subject of several applications as glazing material for solar collectors **[TB1]**. Part of the radiation is absorbed by the plate depending on its optical properties. Thus, the wall behind the plate in turn receives a part of the solar radiation and is heated in turn. The air ascending through the plenum gets warmer in contact with this wall. This air is drawn into the building via a fan.

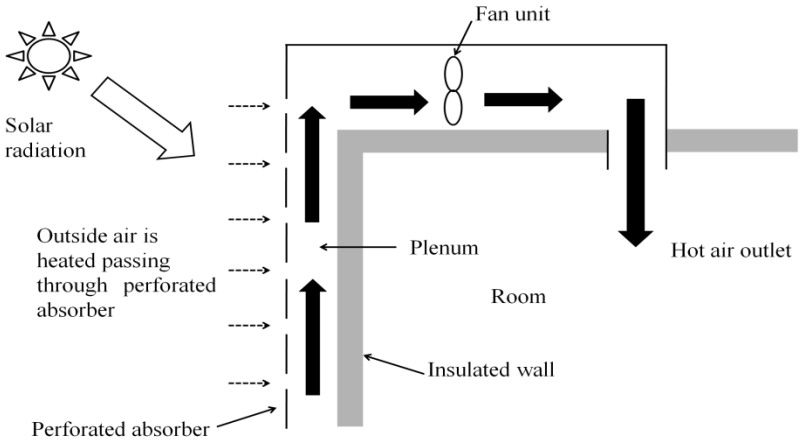


**Figure1: Schematic of the TTC configuration.**

### 2.2-Assumptions

The following assumptions are considered in TTC modeling:

(i) From the viewpoint of convection between the semitransparent plate and the air passing through the transparent plate behaves like the one passing through a UTC at the temperature of plate. The fact that the thickness of plate and that the conductivity thereof very little influence the effectiveness of UTC **[K1]** strengthens the formulation of this hypothesis;

(ii) Heat exchange by convection is considered to be identical over the entire surface of the collector. This assumption is required for a simple model and found to realistic in the past **[KC1]**;

(iii) The suction and air flow phenomena through the transparent plate and into the plenum are considered identical to those of UTC **[G1]**;

(iv) Heat loss by convection between the plate and the environment are neglected, because this is observed for UTC in suction appropriate conditions **[K1]**. Since the plate of a TTC is semi-transparent, its absorbency is lower than that of a UTC and therefore its temperature will necessarily be less than that of a UTC subject to the same conditions, this assumption is valid **[G1]**;

(v) The flow rate through the plate is considered as a constant and homogeneous over the entire perforated plate;

(vi) The flow is directed from the exterior to the plenum through the perforated plate then of plenum towards the outlet of collector of without flow reversal.

### 2.3-Energy balance equations

The different transfer modes that govern the operation of TTC are illustrated in Figures 2 and 3 in order to predict its thermal performance. The balance equations are established for semitransparent perforated plate, the plenum, the wall and the collector.

#### 2.3.1-Transparent perforated plate

Figure 2.a summarizes the exchange of flux at the plate. The equation expressing the different transfers presents only the net radiation balance in order not to burden schematics and equations. Thus, the energy balance on the plaque can be written as follows:

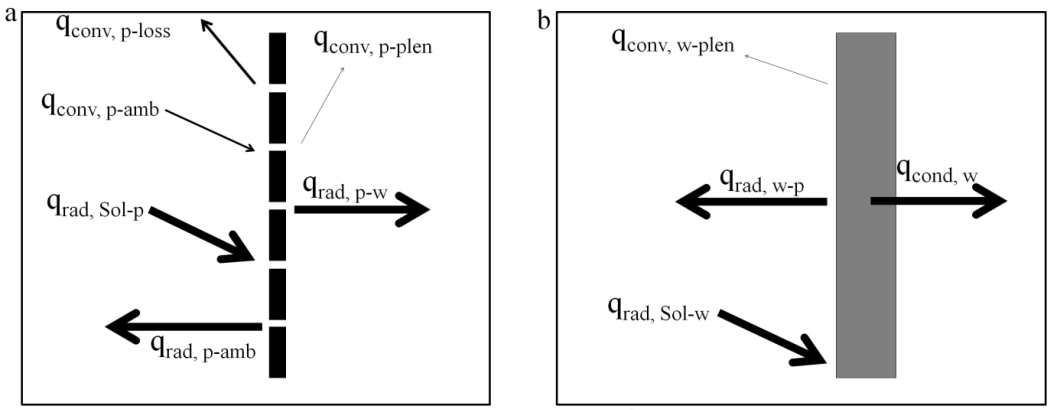


**Figure 2: Heat balance: (a) On transparent perforated plate. (b) On wall.**

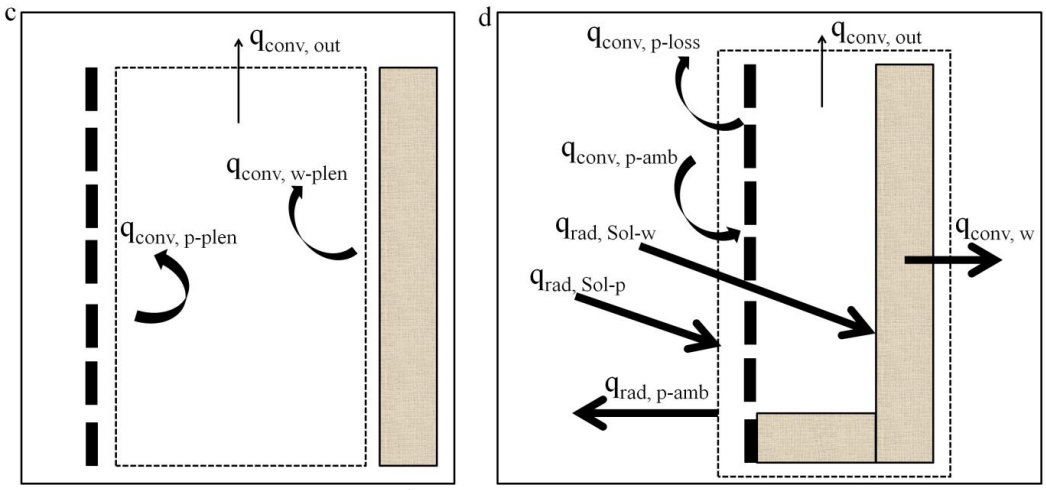


**Figure 3: Heat balance: (c) Balance the airflow passing through the plenum. (d) Global balance on collector**

$$q_{rad,Sol-p} - q_{rad,p-w} - q_{rad,p-amb} + q_{conv,p-amb} - q_{conv,p-loss} - q_{conv,p-plen} = 0 \quad (1)$$

The expressions of terms calculated in the balance sheet on plate are the following:

$$q_{rad,Sol-p} = \alpha_{eff,p} A_T G_{Sol} \quad (2)$$

$$\text{Where } \alpha_{eff,p} = \alpha_p + \alpha_p \tau_p \rho_w \frac{1}{1-\rho_w \rho_p} \quad (3)$$

$$q_{rad,p-w} = \varepsilon_{eff,p-w} \tilde{\sigma} A_T \left(T_p^4 - T_w^4\right) \quad (4)$$

$$\text{Where } \varepsilon_{eff,p-w} = 1/\left((1/\varepsilon_w + 1/\varepsilon_p) - 1\right) \quad (5)$$

$$q_{rad,p-amb} = \varepsilon_{eff,p-amb} \tilde{\sigma} A_T \left(T_p^4 - T_{amb}^4\right) \quad (6)$$

The perforated plate is directly exposed to the environment which is considered as a black surface. The view factor between the plate and the environment is therefore 1 and the effective emissivity between the plate and the environment becomes:

$$\varepsilon_{eff,p-amb} = \varepsilon_p \quad (7)$$

$$q_{conv,p-amb} = \dot{m}_{amb} c_{\bar{p},amb} T_{amb} \quad (8)$$

$$q_{conv,p-plen} = \dot{m}_{in} c_{\bar{p},in} T_{in} \quad (9)$$

By assumption,

$$q_{conv,p-loss} = 0 \quad (10)$$

Thus on plate:

$$\alpha_{eff,p} A G_{Sol} - \varepsilon_{eff,w-p} \tilde{\sigma} A_T \left(T_p^4 - T_w^4\right) - \varepsilon_{eff,p-amb} \tilde{\sigma} A_T \left(T_p^4 - T_{amb}^4\right) - \dot{m}_{in} \left(c_{\bar{p},in} T_{in} - c_{\bar{p},amb} T_{amb}\right) = 0 \quad (11)$$

### 2.3.2-Energy balance on wall

On figure 2b are shown the different heat transfer flows at the wall. The heat balance is written as follows:

$$q_{rad,Sol-w} - q_{conv,w-plen} - q_{rad,w-p} - q_{cond,w} = 0 \quad (12)$$

The empirical correlation reported by **[K1]** is used in the present model to estimate the Nusselt number.
The Nusselt number for conversion heat transfer between the plenum air and wall,

$$Nu_w = 0.664 * (\mathrm{Re}_w)^{0.5} * (\mathrm{Pr}_w)^{0.333} \quad (13)$$

Where

$$\mathrm{Re}_w = (\rho_{air} * v_{plen} * H) / \mu_{air} \quad (14)$$

$$\mathrm{Pr}_w = (c_{\bar{p},in} * \mu_{air}) / K_{air} \quad (15)$$

The convective heat transfer coefficient between the plenum air and wall is estimated from

$$h_w = (Nu_w * K_{air}) / d_{plen} \quad (16)$$

The different terms involved in the equation (9) are calculated as follows:

$$q_{rad,Sol-w} = \alpha_{eff,w} A_T G_{Sol} \quad (17)$$

$$q_{conv,w-plen} = h_w A_T (T_w - T_{plen}) \quad (18)$$

$$q_{rad,w-p} = \varepsilon_{eff,w-p} \tilde{\sigma} A_T (T_w^4 - T_p^4) \quad (19)$$

By assumption, $q_{cond,w} = 0$ (20)

Where $\varepsilon_{eff,w} = \alpha_w \tau_p / (1 - \rho_w \rho_p)$ (21)

The energy balance on wall:

$$\varepsilon_{eff,w} A_T G_{Sol} - h_w A_T (T_w - T_{plen}) - \varepsilon_{eff,w-p} \tilde{\sigma} A_T (T_w^4 - T_p^4) = 0 \quad (22)$$

### 2.3.3-Plenum air

From the Figure 3.a, the energy balance of plenum is:

$$q_{conv,p-plen} + q_{conv,w-plen} - q_{conv,out} = 0 \quad (23)$$

The terms involved in the equation (23) can be expressed as follows:

$$q_{conv,out} = \dot{m}_{out} c_{\bar{p},out} T_{out} \quad (24)$$

$$q_{conv,p-plen} = \dot{m}_{in} c_{\bar{p},in} T_{in} \quad (25)$$

$$q_{conv,w-plen} = h_w A_T (T_w - T_{plen}) \quad (26)$$

The energy balance of the plenum becomes:

$$\dot{m}_{in} c_{\bar{p},in} T_{in} + h_w A_T (T_w - T_{plen}) - \dot{m}_{out} c_{\bar{p},out} T_{out} = 0 \quad (27)$$

### 2.3.4-Total energy balance on collector

The balance on the collector, illustrated in Figure 3.b, used to verify the balance and establish the link between the other three balances separately. By performing this total balance, the following expression is obtained:

$$q_{rad,Sol-w} + q_{rad,Sol-p} - q_{rad,p-amb} + q_{conv,p-amb} - q_{conv,p-loss} - q_{conv,out} - q_{cond,w} = 0 \quad (28)$$

Calculate the different terms involved in the equation (28) is presented as follows:

$$q_{rad,Sol-w} = \varepsilon_{eff,w} A_T G_{Sol} \quad (29)$$

$$q_{rad,p-amb} = \varepsilon_{eff,p-amb} \tilde{\sigma} A_T (T_p^4 - T_{amb}^4) \quad (30)$$

$$q_{conv,p-amb} = \dot{m}_{amb} c_{\bar{p},amb} T_{amb} \quad (31)$$

$$q_{rad,out} = \dot{m}_{out} c_{\bar{p},out} T_{out} \quad (32)$$

$$q_{conv,loss} = 0 \quad (33)$$

$$q_{conv,w} = 0 \quad (34)$$

The flows $q_{rad,Sol-w}$ is represented as crossing the border of collector because he is absorbed by the wall.
Thus, the balance all over collector is written:

$$(\alpha_{eff,w} + \alpha_{eff,p}) A_T G_{Sol} - \varepsilon_{eff,p-amb} \tilde{\sigma} A_T (T_p^4 - T_{amb}^4) + \dot{m}_{amb} c_{\bar{p},amb} T_{amb} - \dot{m}_{out} c_{\bar{p},out} T_{out} = 0 \quad (35)$$

The previously established relationships allow eg to determine some performance criteria of system such as the collector efficiency $\eta$, the temperature difference $\Delta T$ between the environment and the outlet of collector and finally the net heat transfer rate recovered $q_{out}$. The expressions allowing to calculate these criteria are as follows

$$\eta = \frac{\dot{m}_{out} c_{\bar{p},out} T_{out} - \dot{m}_{amb} c_{\bar{p},amb} T_{amb}}{A_T G_{Sol}} \quad (36)$$

$$\Delta T = T_{out} - T_{amb} \quad (37)$$

$$q_{out} = \dot{m}_{out} c_{\bar{p},out} T_{out} - \dot{m}_{amb} c_{\bar{p},amb} T_{amb} \quad (38)$$

### 2.4-Air Properties **[MA1]**

The thermophysical properties of air are calculated from polynomial curve fits to a data set in **[ID1]** for convenience in programming. They can be written in the form of $AT^4 + BT^3 + CT^2 + DT + E$ with their constants are

found in Table 1. Also the air density can be obtained from $\rho = 360.7782\,T^{-1.00336}$ (kg/m$^3$)

**Table 1: Properties of air**

| | $A$ | $B$ | $C$ | $D$ | $E$ |
|---|---|---|---|---|---|
| $c_{\bar{p},in}$ | 1.933E-10 | -7.999E-07 | 1.141E-03 | -4.489E-01 | 1.058E+03 |
| $\nu$ | 0 | -1.156E-14 | 9.573E-11 | 3.760E-08 | -3.448E-06 |
| $K$ | 0 | 1.521E-11 | -4.857E-08 | 1.018E-04 | -3.933E-04 |
| $\alpha_T$ | 0 | 0 | 9.102E-11 | 8.820E-08 | -1.065E-05 |

### 2.5-Models of the rates of satisfaction

The different criteria used in this study are not the same size. To solve this problem of scaling, desirability functions for transforming the variables dimensionless criteria are tapped. But the choice of a desirability function depends on the requirements of the study to be conducted. In our case, the

temperature difference is minimized and efficiency is maximized as shown in Table 2. For this purpose, the function of desirability of Harrington is used **[SQ1]**, **[WT1], [SG1]**:

Minimization function

$$d(Y_m) = \exp(-\exp(b_1 + a_1.Y_m))$$

$$\text{With } a_1 = \frac{\ln(\ln(0.01)/\ln(0.99))}{AUC - USL}, \quad (39)$$

$$b_1 = \ln(-\ln(0.99)) - \alpha.USL$$

Maximization function

$$d(Y_m) = \exp(-\exp(b_2 + a_2.Y_m))$$

$$\text{With } a_2 = \frac{\ln(\ln(0.99)/\ln(0.01))}{LSL - ALC}, \quad (40)$$

$$b_2 = \ln(-\ln(0.99)) - a_2.LSL$$

Levels of criteria are summarized in Table 2.

**Table 2: Levels of criteria**

| Criteria | Aim | $USL$ | $AUC$ |
|---|---|---|---|
| $\eta$ | Maximize | 20% | 94% |
| | | $ALC$ | $LSL$ |
| $\Delta T$ | Minimize | $10^{-3}$ K | 0.765 K |

Then, the criteria are aggregated according the aggregation method based on weighted geometric mean of desirability functions **[D1]**. The global desirability function obtained is defined by:

$$OF = \prod_{n=1}^{2} d_n^{w_n}(Y_n) \quad (41)$$

The weights used are essential because they represent the wishes of the user in the implementation of collector. The values of these weights are summarized in Table 3.

**Table 3: Weight Criteria**

| **Criteria** | $\eta$ | $\Delta T$ |
|---|---|---|
| **Weight (%)** | 60% | 40% |

### 2.5-Optimization procedure

The optimization technique used is the systematic scanning approach of design variables (diameter and pitch of the holes) to find the different optimal combinations.
In this study, two criteria are considered. These are:

- $\rightarrow$ inimization the temperature difference $\Delta T$ ;
- $\rightarrow$ aximizing efficiency collector $\eta$

After modeling the problem in our approach to optimize multi-objective can be summarized as follows:

$$\text{Find } x = [D, P]^T$$

$$\text{Which maximize } OF(x) = \{\eta(x), \Delta T(x)\}$$

$$\text{Suject to } 20\% \le \eta(x) \le 90\%$$

$$10^{-3} \le \Delta T \le 0.765 \quad (42)$$

$$12 \le P \le 24$$

$$0.8 \le D \le 1.55$$

($P$ and $D$ in mm). Thus, for different sets of combination of design variables, the corresponding global objective functions are determined. The candidate solutions obtained are ranked in descending order according to their corresponding satisfaction.

## 3-Results and discussions

The study focused on the Cotonou region located south of Benin and having the geographic coordinates: latitude 6°22'N, longitude 2°37'E. The sunshine and temperature data used are those recorded during the month of July 2002 in Cotonou. This is a type month.

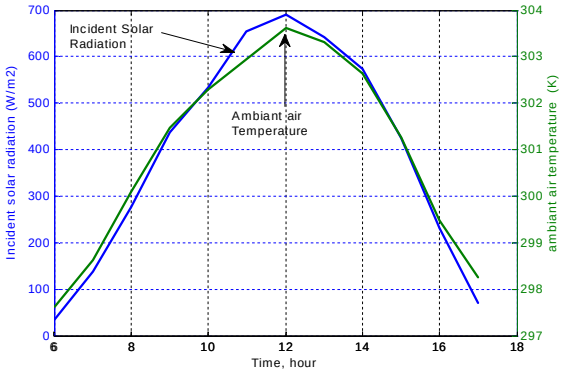


**Figure 4: variation of solar radiation and ambient air temperature**

By analyzing the results presented in Figure 4, we deduce that solar radiation increases with time until a maximum value at about 12 hours then starts to decrease until reaching zero at sunset.

Solving the system of equations by a numerical simulation program MATLAB was used to determine the desired settings from the database. The numerical results obtained make it possible to highlight the effect of several parameters on characteristics of TTC.

Table 4 summarises the input parameters and the range of their values used in the present study. The output parameters estimated were (a) collector efficiency, (b) rate of heat retrieved, and temperature difference. The effect of varying the input parameters on these were also studied.

**Table 4: Physical parameters and numerical fixed**

| Parameter | Value |
|---|---|
| Collector height (m) | 10 |
| Collector length (m) | 2 |
| Hole pitch (mm) | 16 |
| Plate thickness (mm) | 2.8 |
| Schema | square |
| Hole diameter (mm) | 1.2 |
| Plenum depth (cm) | 16 |
| Emissivity of environment | 1 |
| Emissivity of plate | 0.92 |
| Emissivity of wall | 0.92 |
| Reflectivity of plate | 0.08 |
| Ambient Temperature (K) | 271.42 |
| Solar radiation (W/m$^2$) | 400 |

### 3.1-Effect of incident solar radiation on efficiency collector

The degree of performance of solar collector is judged by its efficiency. Figure 5 briefly illustrates the curve of a collector typical efficiency according to sunshine. Logically, we find that the collector efficiency is high when solar radiation is low (eg in cloudy weather).

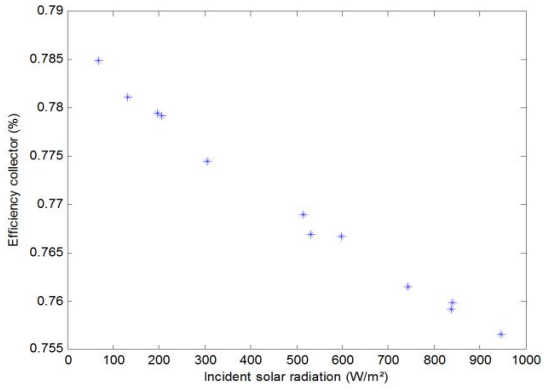


**Figure 5: Variation of collector efficiency as a function of incident solar radiation**

### 3.2-Effect of hole pitch on rate of heat recovered

For a constant diameter, the effect of variation of hole pitch on the amount of recovered heat is insignificant. It is noted that it is especially between 10 hours is 13 hours that the impact of variation of hole pitch is slightly remarkable. Thus, a decrease of hole pitch has the effect an increase the amount of heat. This increase is due to the fact that a decrease in the pitch of the holes increases the number of holes and therefore, the air flow entering the collector is important.

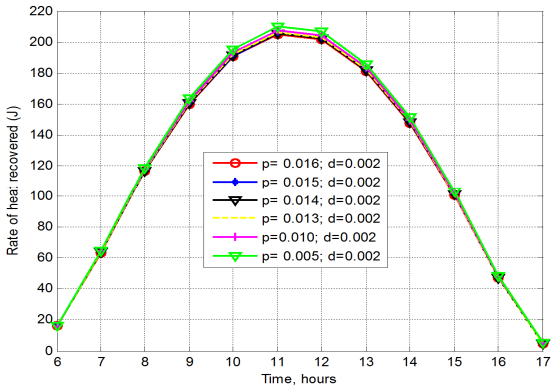


**Figure 6: Variation of rate of heat recovered as a function of hole pitch**

### 3.3 Effect of hole diameter on rate of heat recovered

For a constant hole pitch, the effect of varying the hole diameter on rate of heat recovered is more significant than in the case of Figure 6. Thus, for a reduction of hole diameter 1.2 mm, there is an increase of heat rate of 33.71% (Fig. 7) against an increase of 2.43% for a decrease of 11 mm of hole pitch. The phenomenon observed in Figure 7 can be explained by the fact that a reduction in the diameter of holes leads to a decrease the amount of air coming within the plenum and therefore air will be preheated quickly.

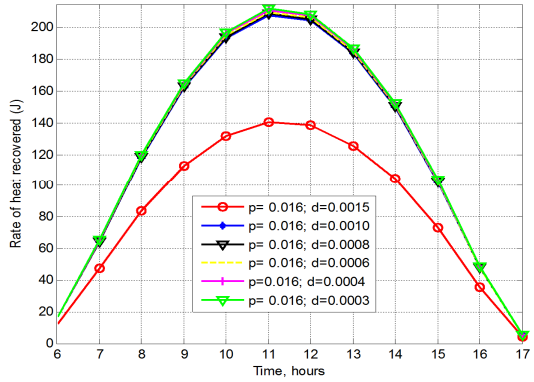


**Figure 7: Variation of rate of heat recovered as a function of diameter pitch**

### 3.4-Effect of combination of hole diameter and hole pitch on temperature difference

Figure 8 shows the contours of temperature difference ($\Delta T$) versus different combinations of hole diameter and hole pitch. On figure, it is noted that the effect of two design variables on temperature difference is not too significant. This can be justified by the fact that it is the non-perforated portion of collector that converts solar radiation into heat. In the range of variation of hole diameter and hole pitch, the minimum and maximum values of temperature difference are respectively 0.5959 K and 0.6093 K. A decrease hole pitch of 19 mm to 12 mm against an increase of diameter of 0.5 mm to 1.2 mm, generates a temperature decrease of 2.2%. The optimum torque corresponding to minimum value of $\Delta T$ is: $P = 12mm$ et $D = 1.2mm$. Figure 9 is a 3D representation of $\Delta T$ versus different configurations. To each value of $\Delta T$ corresponds a gaming combination of design variables $(P, D)$. Ten values of T and D are treated with respective holes pitches of 1 mm and 0.1 mm. We also see clearly appear the maximum and minimum values of $\Delta T$.

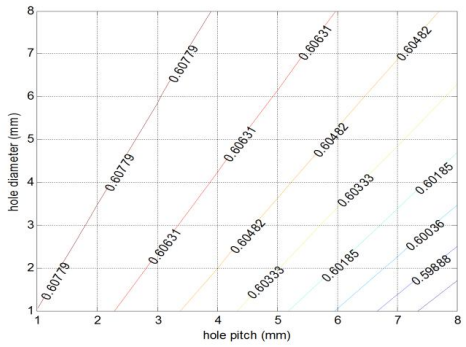


**Figure 8: Temperature difference contours in various hole diameter and hole pitch**

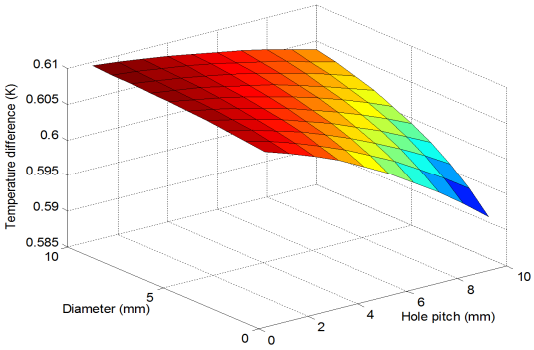


**Figure 9: 3 D representation of $\Delta T$**

### 3.5-Effect of combination of hole diameter and hole pitch on collector efficiency

On Figure 10, we see that the hole diameter and hole pitch have an influence on collector efficiency but less pronounced than on temperature difference. Thus, an increase of hole pitch from 12 mm to 21 mm against a decrease of hole diameter from 1.4 mm to 0.5 mm generates an increase of collector efficiency of 1.03%. The optimum torque of whole diameter and hole pitch obtained is $D = 1.4mm$ et $P = 12mm$. The maximum collector efficiency which respects these conditions is $\eta = 84.3\%$. Figure 11 is a 3D representation of collector efficiency versus different configurations. To each value of $\eta$ corresponds a gaming of combination of design variables. Ten P and D values are considered with respective pitches of 1 mm and 0.1 mm. One sees also appear the maximum and minimum values of $\eta$.

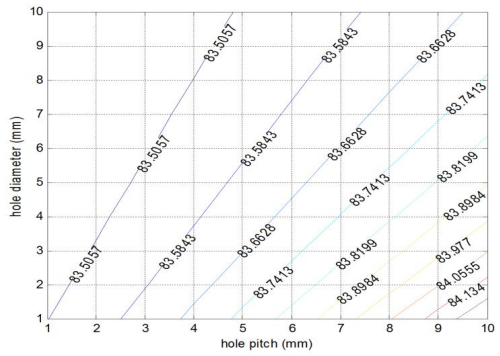


**Figure 10: Collector efficiency contours in various hole diameter and hole pitch**

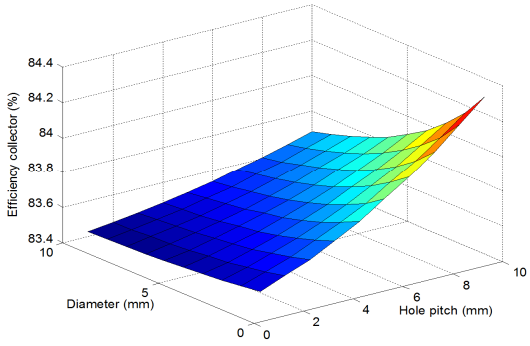


**Figure 11: 3 D representation of $\eta$**

### 3.6-Optimization based on desirability: optimum hole diameter and hole pitch

In the previous sections, the optimization of the collector efficiency and the temperature difference was conducted separately in order to determine $(P,D)$ couples serve firstly of maximizing $\eta$ and partly to minimize $\Delta T$. In this section, the introduction of desirability functions helps determine the Couple $(P,D)$ which minimizes $\Delta T$ without degrading $\eta$. In Figure 12 are plotted contours of global objective function with displaying values. Thus, the optimum configuration corresponds: $P=12mm, D=1.4mm, \eta=84.29\%$, $\Delta T=0.5907K$. Figure 13 shows all the possible solutions and one sees appearing the best solution ie which has the greatest desirability. Table 5 indicate the four best solutions with their characteristics these solutions meet the constraints of problem.

**Tableau 5: Characteristics of four best solutions**

| N° | P (mm) | D (mm) | η (%) | ΔT (K) | OF |
|---|---|---|---|---|---|
| 1 | 12 | 1.4 | 84.29 | 0.5907 | 0.8517 |
| 2 | 12 | 1.3 | 84.16 | 0.5934 | 0.8495 |
| 3 | 13 | 1.4 | 84.15 | 0.5936 | 0.8493 |
| 4 | 12 | 1.2 | 84.05 | 0.5959 | 0.8474 |

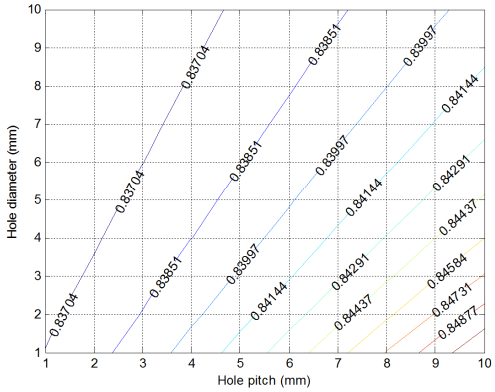


**Figure 12: Contours of global objective function OF**

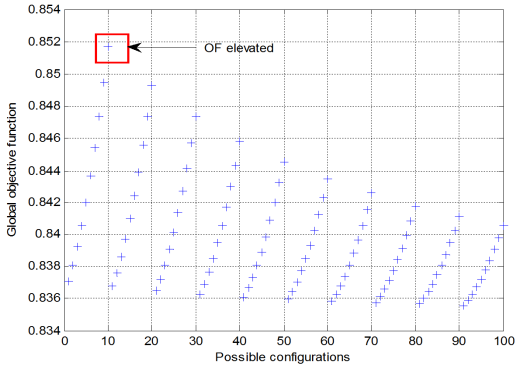


**Figure 13: Evolution of global objective function in various different configurations possible**

## 4. Conclusion

An analysis model of physical phenomena characterizing the TTC was developed. Order to improve the performance of the TTC two objective functions are considered: collector efficiency and temperature difference. The optimization of these two performance criteria is made from two design variables namely the hole diameter and hole pitch. Contours and 3D representations of these functions are also realized. Analysis of results shows that the collector efficiency and the temperature difference are sensitive to the variation of hole pitch and hole diameter. The influence of other parameters such as solar radiation, and hole diameter and hole pitch on recovered heat rate is also discussed.

## References

**[B1]** British Petroleum. 2012. BP Statistical Review of World Energy June 2012. <http://www.bp.com/liveassets/bp_internet/globalbp/globalbp_uk_english/reports_and_publications/statistical_energy_review_2011/STAGING/local_assets/pdf/statistical_review_of_world_energy_full_report_2012.pdf >.

**[BH1]** Badache, M., Hallé, S., Rousse, D. 2012. « A full 34 factorial experimental design for efficiency optimization of

an unglazed transpired solar collector prototype ». Solar Energy, vol. 86, no 9, p. 2802-2810.

**[D1]** Derringer, G. et al., 1980. Stimultaneous optimization of several response variables. JQT, tome 12.

**[G1]** Genevès, C. 2013. « Modélisation unidimensionnelle d'un collecteur solaire aéraulique ». Mémoire de Maîtrise en Génie, Concentration Energies Renouvelables et Efficacité Energétique ; Montréal.

**[ID1]** Incropera, F. P., DeWitt, D. P., Bergman, T. L., Lavine, A. S. (2007). « Fundamentals of Heat and Mass Transfer, 6thed ». New York, NY: John Wiley & Sons Inc.

**[K1]** Kutscher, C. F. 1994. « Heat-exchange effectiveness and pressure-drop for air-fow through perforated plates with and without crosswind ». Journal of Heat Transfer-Transactions of the Asme, vol. 116, no 2, p. 391-399.

**[KC1]** Kutscher, C. F., Christensen, C. B. and G. M. Barker. 1993. « Unglazed transpired solar collectors - heat-loss theory ». Journal of Solar Energy Engineering-Transactions of the Asme, vol. 115, no 3, p. 182-188.

**[MA1]** Motahar, Sadegh, et Ali Akbar Alemrajabi. 2010. « An analysis of unglazed transpired solar collectors based on exergetic performance criteria ». International Journal of Thermodynamics, vol. 13, no 4, p. 153-160.

**[S1]** Sèmassou, C. 2011. « Aide à la décision pour le choix de sites et systèmes énergétiques adaptés aux besoins du Bénin ». Thèse de doctorat, Université Bordeaux 1.**[SG1]** Semassou, G. C., Guidi, T. C., Dangbédji, C., Degan, G., 2015. Optimal design of a wind system for water pumping using a genetic algorithm. Vestnik Mezhdunarodnoi Akademii Kholoda, N°2.

**[SQ1]** Sebastian, P., Quirante, T., Ho Kon Tiat, V., Ledoux, Y., 2010. Multi-objective optimization of the design of two-stage flash evaporators: Part 2. Multi-objective optimization. International Journal of Thermal Sciences 49, 2459-2466.

**[TB1]** Tjandraatmadja, G.F., Burn L.S., and Jollands M.C., Evaluation of commercial polycarbonate optical properties after QUV-A radiation—the role of humidity in photodegradation. Polymer Degradation and Stability, 78(3): p. 435-448, (2002).

**[WT1]** Wagner, T., Trautmann, H., 2010. Integration of preferences in hypervolume-based multi-objective evolutionary algorithms by means of desirability functions. IEE transactions on evolutionary computation, vol.14, N°5.

## Annexe

**Nomenclature**

| | | | |
|---|---|---|---|
| $A_T$ | total collector area (m²) | $q_{conv,p-amb}$ | convection heat transfer from air to plate (W) |
| $ALC$ | absolute lower cutoff | $q_{conv,p-plen}$ | transfer by convection of outgoing plate and entering the plenum (W) |
| $AUC$ | absolute upper cutoff | $q_{conv,p-amb}$ | convection heat transfer from air to plate (W) |
| $c_{\bar{p},in}$ | specific heat of air coming out of plate and entering the plenum (J/kg.K) | $q_{conv,p-plen}$ | transfer by convection of outgoing plate and entering the plenum (W) |
| $c_{\bar{p},out}$ | exit air specific heat of plenum (J/kg.K) | $q_{conv,p-loss}$ | convective losses between the plate and the ambient (W) |
| $D$ | perforation diameter (m) | $q_{conv,w-plen}$ | convective transfer from wall to air plenum (W) |
| $d$ | desirability | $q_{out}$ | net rate of heat recovered (J) |
| $d_{plen}$ | plenum depth (m) | $q_{rad,Sol-p}$ | solar radiation absorbed by the semi-transparent plate (W) |
| $G_{Sol}$ | incident solar radiation (W/m²) | $q_{rad,Sol-w}$ | solar radiative transfer absorbed by the wall (W) |
| $H$ | collector height (m) | $q_{rad,p-amb}$ | net radiative transfer between the plate and the ambient (W) |
| $K_{air}$ | thermal conductivity of air (W/m K) | $q_{rad,w-p}$ | radiative transfer from the wall to plate (W) |
| $LSL$ | lower soft limit | $\mathrm{Re}_w$ | reynolds number on wall |
| $\dot{m}_{amb}$ | mass flow rate of air through the collector (kg/s) | $T_{amb}$ | ambient air temperature |
| $\dot{m}_{in}$ | mass flow rate from perforated plate to plenum (kg/s) | $T_{\mathrm{int}}$ | air temperature leaving the perforated plate and entering the plenum (K) |

 

| | | | |
|---|---|---|---|
| $\dot{m}_{out}$ | exit air mass flow of plenum (kg/s) | $T_{out}$ | exit air temperature of plenum (K) |
| $OF$ | global desirability function | $T_p$ | temperature of plate (K) |
| $P$ | pitch of perforations (m) | $T_w$ | temperature of wall (K) |
| $\mathrm{Pr}_w$ | prandtl number on wall | $USL$ | upper soft limit for the criterion |
| $q_{cond,w}$ | transfer by conduction of wall with inside the building (W) | $w_n$ | weights |
| $q_{conv,out}$ | exit convective transfer of collector (W) | $Y_m$ | criterion |
| **Greek symbols** | | | |
| $\alpha_{eff,p}$ | effective absorptivity of plate | $\eta$ | efficiency collector |
| $\alpha_p$ | absorptivity of plate | $\rho_{air}$ | density of air (kg/m$^3$) |
| $\alpha_T$ | thermal diffusivity (m$^2$/s) | $\rho_p$ | reflectivity of plate |
| $\alpha_w$ | absorptivity of wall | $\rho_w$ | reflectivity of wall |
| $\Delta T$ | temperature difference (K) | $\hat{\sigma}$ | Stephan Boltzmann Constant (5.67.10$^{-8}$ Wm$^{-2}$K$^{-4}$) |
| $\varepsilon_{eff,p-amb}$ | effective emissivity between the plate and the ambient | $\nu_{plen}$ | kinematic viscosity (m$^2$/s) |
| $\varepsilon_{eff,p-w}$ | effective emissivity between the plate and the wall | $\mu_{air}$ | dynamic viscosity of air (kg/ms) |
| $\varepsilon_p$ | emissivity of plate | $\tau_p$ | transmissivity of plate |
| $\varepsilon_w$ | emissivity of wall | | |

 